

See discussions, stats, and author profiles for this publication at: <https://www.researchgate.net/publication/51603037>

Synthesis of Graphene Nanoribbons Encapsulated in Single-Walled Carbon Nanotubes

ARTICLE in NANO LETTERS · SEPTEMBER 2011

Impact Factor: 13.59 · DOI: 10.1021/nl2024678 · Source: PubMed

CITATIONS

76

READS

74

7 AUTHORS, INCLUDING:



Alexandr V Talyzin

Umeå University

126 PUBLICATIONS 1,474 CITATIONS

SEE PROFILE



Ilya V. Anoshkin

Aalto University

64 PUBLICATIONS 466 CITATIONS

SEE PROFILE



Risto M Nieminen

Aalto University

623 PUBLICATIONS 18,819 CITATIONS

SEE PROFILE



Albert G Nasibulin

Skolkovo Institute of Science and Technology

231 PUBLICATIONS 3,837 CITATIONS

SEE PROFILE

Synthesis of Graphene Nanoribbons Encapsulated in Single-Walled Carbon Nanotubes

Alexandr V. Talyzin,^{*,†,⊥} Ilya V. Anoshkin,^{*,†,⊥} Arkady V. Krashenninnikov,^{§,||} Risto M. Nieminen,^{||} Albert G. Nasibulin,[‡] Hua Jiang,[‡] and Esko I. Kauppinen[‡]

[†]Department of Physics, Umeå University, S-90187 Umeå, Sweden

[‡]NanoMaterials Group, Department of Applied Physics and Center for New Materials, Aalto University, P.O. Box 15100, FI-00076 Aalto, Espoo, Finland

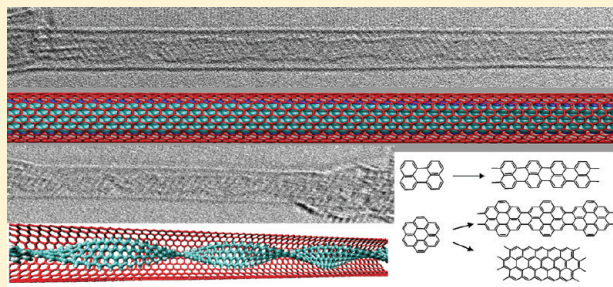
[§]Department of Physics, University of Helsinki, P.O. Box 43, FI-00014 Helsinki, Finland

^{||}COMP/Applied Physics, Aalto University, P.O. Box 1100, FI-00076 Aalto, Finland

S Supporting Information

ABSTRACT: A novel material, graphene nanoribbons encapsulated in single-walled carbon nanotubes (GNR@SWNT), was synthesized using confined polymerization and fusion of polycyclic aromatic hydrocarbon (PAH) molecules. Formation of the GNR is possible due to confinement effects provided by the one-dimensional space inside nanotubes, which helps to align coronene or perylene molecules edge to edge to achieve dimerization and oligomerization of the molecules into long nanoribbons. Almost 100% filling of SWNT with GNR is achieved while nanoribbon length is limited only by the length of the encapsulating nanotube. The PAH fusion reaction provides a very simple and easily scalable method to synthesize GNR@SWNT in macroscopic amounts. First-principle simulations indicate that encapsulation of the GNRs is energetically favorable and that the electronic structure of the encapsulated GNRs is the same as for the free-standing ones, pointing to possible applications of the GNR@SWNT structures in photonics and nanoelectronics.

KEYWORDS: Graphene, graphene nanoribbons, carbon nanotubes, SWNT, polycyclic aromatic hydrocarbons



Graphene nanoribbons (GNRs) are of great interest for various applications due to their unique electronic properties that can be modified by altering their width and geometry.^{1–10} Several methods have recently been proposed for GNR synthesis, for example, unzipping of carbon nanotubes^{1,11–14} or cutting two-dimensional (2D) graphene sheets to ribbons by electron¹⁵ or ions beams.¹⁶ GNRs have also been produced using deposition and fusion reaction of hydrocarbons on metallic surfaces.^{3,15,17,18} Here we demonstrate a very simple and efficient method for synthesis of hydrogen-terminated graphene nanoribbons encapsulated in single-walled carbon nanotubes (SWNTs) using thermally induced fusion of coronene and perylene molecules. Carbon nanotubes in this reaction provided one-dimensional alignment of molecules required for the fusion reaction into graphene nanoribbons. Almost 100% filling of SWNTs was achieved, while the choice of the precursor allows to modify the shape of nanoribbons.

Coronene is a large polycyclic aromatic hydrocarbon (PAH) molecule which consists of six carbon hexagons fused into a ring whereas perylene consists of five hexagon rings.¹⁹ These materials are available in macroscopic amounts, soluble in common solvents (e.g., toluene) and can easily be sublimated.²⁰ Coronene was considered in many theoretical studies^{21,22} as a model for nanographene terminated by hydrogen. It is well-known that annealing of coronene at certain temperatures leads to fusion

reaction with the formation of coronene dimer-dicoronylene.^{21,22} Fusion of several coronene molecules was suggested as a road to formation of progressively larger graphene flakes. Although only trimers and tetramers were detected using mass spectrometry²³ in previous experiments, a steplike fusion reaction leading to formation of larger PAHs was recently confirmed.²⁰ The study suggested to impose geometrical restrictions for the alignment of coronene (or other PAH) molecules prior to thermal fusion to synthesize the GNRs. This can be achieved if SWNT is used as a one-dimensional (1D) reactor for the insertion and fusion of PAH molecules. Our experiments indeed demonstrated that coronene and perylene molecules can be polymerized and fused into graphene nanoribbons due to the effect of one-dimensional aligning inside of SWNTs.

In order to synthesize GNRs, SWNTs opened by oxidation treatment were exposed to coronene or perylene vapor in reactors sealed with argon at ambient pressure. Typically, annealing was performed for 1–24 h in the temperature range starting from just above the melting point of coronene (438 °C) up to the temperatures at which bulk coronene fusion reactions were observed

Received: July 19, 2011

Revised: August 14, 2011

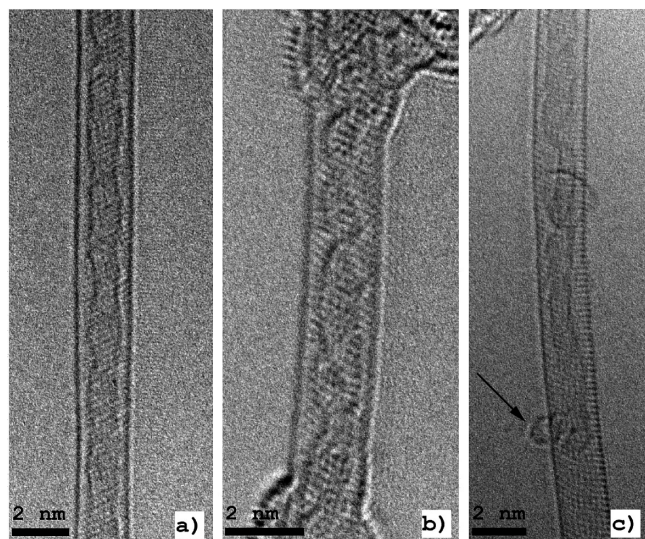


Figure 1. TEM images of GNRs encapsulated in SWNT (a,b) obtained using coronene precursor and (c) obtained using perylene precursor. Molecule of perylene (0.8 nm in diameter) is also visible on outer surface of SWNT (marked by arrow).

previously (530 °C).²⁰ Perylene/SWNT samples were annealed in the temperature range of 350–450 °C with best results obtained at 400 °C.

Surprisingly, formation of GNRs encapsulated in SWNT (GNR@SWNT) was observed for the whole temperature interval above the melting point of coronene, even for temperatures significantly lower than the previously established temperature of the reaction in free (not encapsulated in nanotubes) vapor (above 530 °C).²⁰ Typical images of GNR@SWNT are shown in Figure 1. At higher temperatures (470–530 °C), coronene oligomers precipitated not only inside, but also outside carbon nanotubes, which complicated the analysis, since the products are not soluble in toluene and do not sublime.²⁰ The sample annealed at 530 °C was so strongly contaminated by carbon precipitates that observation of nanotubes by high-resolution electron microscopy (HRTEM) was not possible. However, at 450–470 °C most of the material precipitated outside SWNTs could be removed by thermal treatment and dissolving in toluene. Analysis of the HRTEM images collected from these samples showed that GNRs are formed inside SWNTs with almost 100% filling, and that the length of nanoribbons was limited only by the length of the nanotubes (Figure 1a,b). The nanoribbons were often nonuniform in the width with a visible variation in width in the range of ~0.5–1.0 nm (nanotube diameter ~1.7–2.0 nm) (Figure 1a,b). The maximal width of GNRs is limited by the diameter of the SWNTs while the geometrical shape is more complicated. The nanoribbons were observed to twist and to form helical configurations in many places (Figure 1b), but in a rather different way compared to helices predicted in recent theoretical work.^{24,25} It is interesting to note that SWNT bundles contain encapsulated GNRs aligned in one direction provided by orientation of the bundle which could be useful for some applications. Alignment of GNRs in one direction could help, for example, to study their magnetic properties, conductivity, or heat transport. Very similar but somewhat narrower and more strongly twisted nanoribbons were also obtained using perylene precursor (Figure 1c).

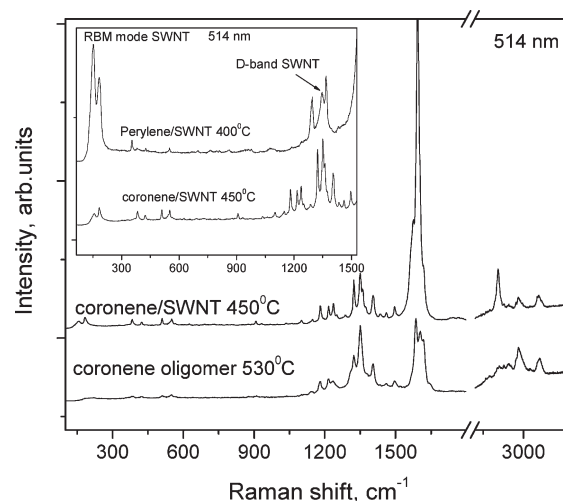


Figure 2. Raman spectra of oligomer formed by annealing of coronene powder at 530 °C compared to the spectra of GNR@SWNT sample obtained using coronene precursor at 450 °C. Inset shows zoomed part of Raman spectra recorded from GNR@SWNT obtained using coronene and perylene as precursors.

It should be noted that the excess of coronene (perylene) powders loaded in the containers remained unchanged (unpolymerized) after annealing at 450–490 °C for coronene and 400 °C for perylene. Only the molecules that were inserted into the SWNTs or positioned on their surface reacted with each other. Obviously, SWNTs serve as nucleation centers for coronene (perylene) fusion and catalyze the reaction that results in the formation of bulk hydrocarbon products on the outer side of SWNTs and GNRs inside the SWNTs. Therefore, the aligning effect of one-dimensional space inside nanotubes on the orientation of the inserted coronene molecules is crucial for the formation of the nanoribbons. Since coronene and perylene are molecules terminated by hydrogen atoms, it is expected that nanoribbons formed inside SWNTs are also hydrogen-terminated. Evidence for hydrogen termination can be found in Raman spectra of GNR@SWNT samples (Figure 2).

Formation of GNR@SWNT in macroscopic amounts was confirmed by Raman spectra recorded from the samples annealed in the presence of coronene or perylene vapors (Figure 2). The spectra also demonstrate that the nanoribbons obtained using perylene and coronene are significantly different. Figure 2 shows the spectrum of a toluene-washed sample of SWNTs annealed in coronene vapor at 450 °C, as compared to the spectrum obtained in our previous study from coronene oligomer powder obtained at 530 °C.²⁰ The Raman peaks that originate from SWNTs remain almost unchanged compared to those corresponding to the pristine nanotubes, while a number of additional peaks from coronene oligomers are found in the spectrum. Very similar spectra were also recorded from the samples thermally treated at 470 and 490 °C indicating similar reaction pathway. The Raman spectra also clearly demonstrate that molecules formed by coronene fusion are hydrogen terminated. A number of peaks observed above 2500 cm⁻¹ originate from the region of C–H stretching vibrations. The inset shows spectra of nanoribbons synthesized using coronene and perylene, with obviously very distinct series of peaks. In addition to the SWNT peaks, the perylene/SWNT sample exhibited strong Raman peaks at 1366, 1292 and weaker peaks at 548 and 353 cm⁻¹. The positions of these peaks are very

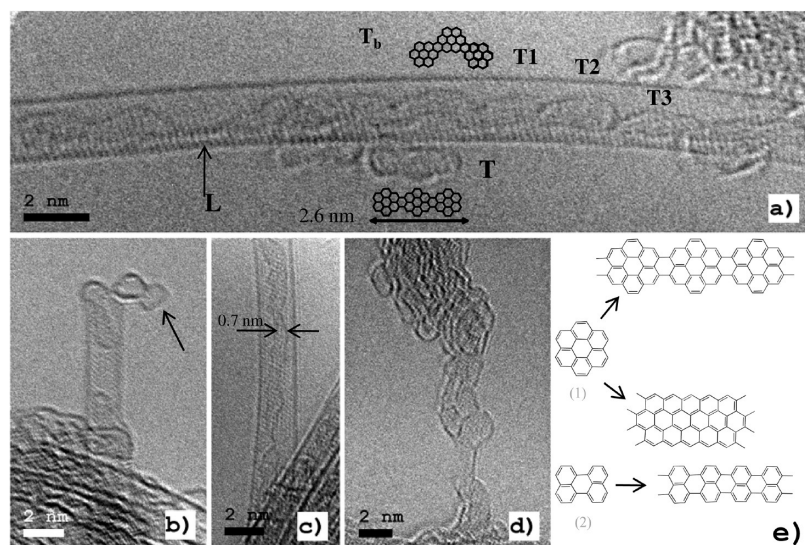


Figure 3. TEM images from coronene/SWNT samples (a) GNR@SWNT formed at 420 °C with coronene trimer on the outer side of nanotube and consecutive chain of trimers (marked T1, T2, T3) inside of SWNT. While the most of the GNR is oriented with in plane of the image, there is a fragment (marked by arrow L) visible from the edge side. The tube-to-ribbon distance is ~ 0.4 nm in this place. (b) Nanotube tip with attached dicoronylene molecule outside and short nanoribbon inside. (c) Nanoribbon that looks rather narrow visible width (~ 0.7 nm) due to orientation away from the image plane. (d) Platelets of large PAHs (nanographenes) with 2–3 nm diameter size formed as a result of coronene fusion on the surface of SWNT at 490 °C sample; (e) Suggested structures of nanoribbons formed using coronene (1) and perylene (2) precursors. Scale bar in all images is 2 nm.

close to those from GNRs described previously as polyperinaphthalene ($1370, 1290\text{ cm}^{-1}$),¹ which is, in fact, the narrowest possible armchair nanoribbon.²⁵

The structure of the nanoribbons produced using coronene as precursor was studied in more detail by varying the reaction temperature over wider range. Surprisingly, we did not observe the stacked coronene columns reported previously²⁶ even when the temperature of reaction was lowered below the melting point of coronene (420 °C). However, the images taken from the samples annealed at lower temperatures revealed intermediate steps of nanoribbons formation (see Figure 3). The chemical bottom-up synthesis of GNRs inside SWNTs can be followed by analyzing the images taken from samples prepared at various temperatures. Figure 3a shows GNR@SWNT formed at 420 °C, which clearly consists of connected molecular blocks. The molecule found on the outer surface of this nanotube is interpreted as a coronene trimer taking into account its shape and dimensions. This molecule was easily removed by the electron beam and not found on the next images. Similar trimer molecules connected as building blocks inside nanotubes are marked as T1, T2, T3. Trimers can also be formed from coronene in a nonlinear configuration, forming bended nanoribbons (see nanoribbon fragment T_b in Figure 3a). The nanoribbon is also twisted in several places. A particularly interesting fragment is marked by arrow L. GNR is oriented perpendicular to the plane of the image, representing a view from the edge. This image clearly proves that the object observed inside the SWNT is a nanoribbon. The step by step fusion of coronene molecules is confirmed by direct observation of dicoronylene in some images (Figure 3b). This image shows easily recognizable dimeric coronene molecule (dicoronylene) with 1.6 nm dimension along the connection axis attached to the nanotube tip, while a similar molecule is inserted into the nanotube inner space.

Nanoribbons can also be identified due to their different orientations inside the nanotube. The very narrow visible width

of some nanoribbons excludes other possible interpretations of the images (Figure 3c). Finally, some nanoribbons were analyzed by taking images at different angles (with a tilt of 30° that also confirmed that the studied object is a nanoribbon (see Supporting materials). The suggested structures of the nanoribbons produced using coronene and perylene precursors are shown in Figure 1e. Figure 3d also demonstrates that fusion of coronene molecules at higher temperatures (490 °C) results in the formation of nanographene platelets on the outer surface of carbon nanotubes. The image shows several platelets with pentagonal or hexagonal shape and diameters in the range 2–3 nm (compared to the 0.8 nm diameter of a coronene molecule). No nanoribbons were found outside of SWNTs. This observation confirms our previous suggestion² that large PAHs can be produced by fusion of coronene molecules, and that nanographene synthesis can be achieved in a similar way.

The role of SWNTs in the GNR formation process was also studied theoretically using density functional theory (DFT) calculations with a nonempirical (without any material-specific parameters) functional for exchange and correlations. This method is capable of describing both short-ranged covalent bonding and long-ranged van der Waals (vdW)-type interaction between the nanotubes and molecules/ribbons inside them. The details of our simulations are given in the Supporting Information. We considered isolated coronene and perylene molecules inside SWNTs, as well as straight ribbons made from these molecules. Armchair (n,n) and zigzag ($n,0$) nanotubes were taken as examples of SWNTs with chiral indices ranging from 9 to 13 and from 14 to 18 for armchair and zigzag tubes, respectively. Our simulations indicated that insertion of the molecules and ribbons into nanotubes is energetically favorable with energy of about 0.2 eV per 1 Å (nanotube length unit) being gained with respect to the isolated systems. The optimum diameter of SWNTs depends on the width of the molecule (ribbon). For example, it is 1.4 nm ((10,10) SWNT) for armchair tubes and

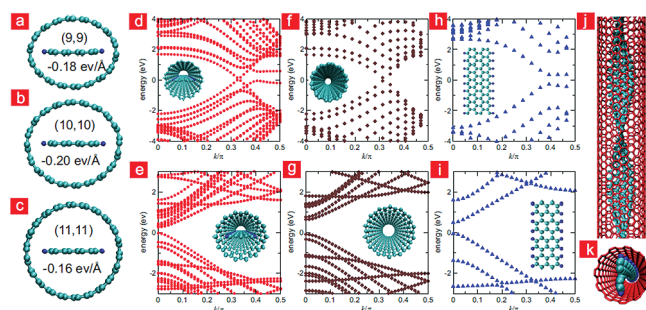


Figure 4. Atomic structure of GNR@SWNTs in the ball-and-stick representation and the electronic structure of the systems as revealed by our first-principles simulations. (a–c) The coronene-based nanoribbons inside armchair nanotubes. The numbers indicate the chiral indices and the vdW-type bonding energy between the ribbon and the nanotube per unit length. (d) Band structure of the coronene-based nanoribbon inside (10,10) nanotube. (e) Band structure of the perylene-based nanoribbon inside (14,0) nanotube. Band structures of the corresponding isolated nanotubes (f,g) and free-standing ribbons (e,h). Top (j) and side (k) views of a twisted coronene-based GNRs inside an armchair nanotube.

coronene-based ribbons, giving the lowest total energy of the system. GNR@SWNT complexes had higher total energy for nanotubes with smaller diameters due to geometrical distortion of the SWNTs (Figure 4a–c), while insertion of the ribbons into nanotubes with larger diameters gives rise to a weaker van der Waals interaction between the tubes and the ribbons.

Our calculations showed that the electronic structure of GNR@SWNT complexes can be understood as a superposition of the electronic structures of the isolated systems, as evidenced by the band structures of the (10,10)-coronene-based ribbon, Figure 4d,e. The electronic properties of the ribbons (e.g., a size-dependent gap value²⁷ and magnetic properties²⁸ are preserved due to a weak noncovalent interaction between the ribbons and the nanotubes. Thus, creation of the stable GNR@SWNT structures in macroscopic amount could possibly lead to use of their unique properties in photonics and nanoelectronics applications.

To conclude, in this study we report a very simple and efficient chemical synthesis method for preparation of a novel material: hydrogen-terminated GNRs encapsulated in SWNTs. Confined polymerization and fusion of PAH molecules from precursor vapor observed inside nanotubes results in differently shaped nanoribbons depending on the precursor used (coronene or perylene). The reaction pathway and temperature conditions are also clearly distinct compared to the bulk powders. This emphasizes that chemistry in 1D space shows significant difference compared to standard reactions in 3D space. Alignment of molecules within inner space of nanotubes promotes formation of nanoribbons while nanotube walls protect them from environment. The material was obtained with almost 100% encapsulation degree, precursors are available in macroscopic amounts, and it is very likely that other PAHs could be used for similar reactions inside nanotubes (possibly not limited to carbon nanotubes). The empty space between nanoribbons and nanotube walls is also sufficient to accommodate additional dopant atoms. This opens a possibility of GNR@SWNT adsorptive doping with, for example, alkali metals, or covalent functionalization of GNRs inside of SWNTs. Various possible combinations of nanotubes and nanoribbons (e.g., metallic GNR inside metallic SWNT or metallic GNR inside semiconducting SWNT, metallic GNR inside of nonconducting

functionalized SWNT, etc.) hold great promise for synthesis of new materials with unusual properties and for their applications.

After the original submission of our manuscript a paper by Chuvilin et al. reporting sulfur terminated short graphene nanoribbons inside of SWNT was published.²⁹ However, the nanoribbons in that study were produced using electron beam under TEM which limits possibility of method to microscopic observations. The bottom to top approach found in our study provides opportunity to make real bulk materials in large variety of modifications and to study their properties.

■ ASSOCIATED CONTENT

S Supporting Information. Details of synthesis and characterization procedures. Additional TEM images of GNR@SWNT, TEM images taken from GNR@SWNT with tilt. Raman spectra recorded using 633 nm laser. Additional figures and data presented for some theoretical results. This material is available free of charge via the Internet at <http://pubs.acs.org>.

■ AUTHOR INFORMATION

Corresponding Author

*E-mail: Alexandr.talyzin@physics.umu.se.

Author Contributions

[†]These authors contributed equally to this work.

■ ACKNOWLEDGMENT

A.T. acknowledges support from Ångpanneföreningens Forskningsstiftelse. This work was partially supported by the Academy of Finland (Project Nos. 128445 and 124283) and TEKES (SIPI 211088 and LIBACAM 211247). We also acknowledge the Finnish IT Center for Science for generous grants of computer time. Personal of Nanomicroscopy Center of Aalto University are acknowledged for help with TEM. Professor B. Sundqvist is acknowledged for proofreading of the manuscript.

■ REFERENCES

- (1) Kosynkin, D. V.; Higginbotham, A. L.; Sinitskii, A.; Lomeda, J. R.; Dimiev, A.; Price, B. K.; Tour, J. M. *Nature* **2009**, *458*, 872.
- (2) Jiao, L. Y.; Zhang, L.; Wang, X. R.; Diankov, G.; Dai, H. J. *Nature* **2009**, *458*, 877.
- (3) Cai, J. M.; Ruffieux, P.; Jaafar, R.; Bieri, M.; Braun, T.; Blankenburg, S.; Muoth, M.; Seitsonen, A. P.; Saleh, M.; Feng, X. L.; Mullen, K.; Fasel, R. *Nature* **2010**, *466*, 470.
- (4) Jiao, L. Y.; Wang, X. R.; Diankov, G.; Wang, H. L.; Dai, H. J. *Nat. Nanotechnol.* **2010**, *5*, 321.
- (5) Shimizu, T.; Haruyama, J.; Marcano, D. C.; Kosynkin, D. V.; Tour, J. M.; Hirose, K.; Suenaga, K. *Nat. Nanotechnol.* **2011**, *6*, 45.
- (6) Hirsch, A. *Angew. Chem., Int. Ed.* **2009**, *48*, 6594.
- (7) Balandin, A. A.; Ghosh, S.; Bao, W. Z.; Calizo, I.; Teweldebrhan, D.; Miao, F.; Lau, C. N. *Nano Lett.* **2008**, *8*, 902.
- (8) Dai, H. J.; Jiao, L. J.; L., Y.; Zhang, L.; Wang, X. R.; Diankov, G. *Nature* **2009**, *458*, 877.
- (9) Ritter, K. A.; Lyding, J. W. *Nat. Mater.* **2009**, *8*, 235.
- (10) Shimizu, T. S.; Haruyama, J.; Marcano, D. C.; Kosynkin, D. V.; Tour, J. M.; Hirose, K.; Suenaga, K. *Nat. Nanotechnol.* **2011**, *6*, 45.
- (11) Bai, J. W.; Cheng, R.; Xiu, F. X.; Liao, L.; Wang, M. S.; Shailos, A.; Wang, K. L.; Huang, Y.; Duan, X. F. *Nat. Nanotechnol.* **2010**, *5*, 655.
- (12) Sinitskii, A.; Dimiev, A.; Kosynkin, D. V.; Tour, J. M. *ACS Nano* **2010**, *4*, 5405.

- (13) Jiao, L. J.; L., Y.; Wang, X. R.; Diankov, G.; Wang, H. L.; Dai, H. J. *Nat. Nanotechnol.* **2010**, *5*, 321.
- (14) Sprinkle, M.; Ruan, M.; Hu, Y.; Hankinson, J.; Rubio-Roy, M.; Zhang, B.; Wu, X.; Berger, C.; de Heer, W. A. *Nat. Nanotechnol.* **2010**, *5*, 727.
- (15) Jin, C. H.; Lan, H. P.; Peng, L. M.; Suenaga, K.; Iijima, S. *Phys. Rev. Lett.* **2009**, *102*, 205501.
- (16) Lemme, M. C.; Bell, D. C.; Williams, J. R.; Stern, L. A.; Baugher, B. W. H.; Jarillo-Herrero, P.; Marcus, C. M. *ACS Nano* **2009**, *3*, 2674.
- (17) Treier, M.; Pignedoli, C. A.; Laino, T.; Rieger, R.; Mullen, K.; Passerone, D.; Fasel, R. *Nat. Chem.* **2011**, *3*, 61.
- (18) Diez-Perez, I.; Li, Z. H.; Hihath, J.; Li, J. H.; Zhang, C. Y.; Yang, X. M.; Zang, L.; Dai, Y. J.; Feng, X. L.; Muellen, K.; Tao, N. J. *Nat. Commun.* **2010**, *1*, 31.
- (19) Fawcett, J. K.; Trotter, J. *Proc. R. Soc. London, Ser. A* **1966**, *289*, 366.
- (20) Talyzin, A. V.; Luzan, S. M.; Leifer, L.; Akhtar, S.; Fetzer, J.; Cataldo, F.; Tsybin, Y. O.; Tai, C. V.; Dzwilewski, A.; Moons, E. J. *Phys. Chem. C* **2011**, *115*, 13207–13214.
- (21) Zander, M.; Franke, W. *Chem. Ber./Recl* **1958**, *91*, 2794.
- (22) Goddard, R.; Haenel, M. W.; Herndon, W. C.; Kruger, C.; Zander, M. J. *Am. Chem. Soc.* **1995**, *117*, 30.
- (23) Joblin, C.; Masselon, C.; Boissel, P.; deParseval, P.; Martinovic, S.; Muller, J. F. *Rapid Commun. Mass Spectrum.* **1997**, *11*, 1619.
- (24) Li, H.; Jiang, Y. Y.; Li, Y. F.; Yu, H. Q.; Liew, K. M.; He, Y. Z.; Liu, X. F. *ACS Nano* **2011**, *5*, 2126.
- (25) Sosnowski, M.; Yu, C.; Wang, S. C.; Iqbal, Z. *Synth. Met.* **2008**, *158*, 425.
- (26) Okazaki, T.; Iizumi, Y.; Okubo, S.; Kataura, H.; Liu, Z.; Suenaga, K.; Tahara, Y.; Yudasaka, M.; Okada, S.; Iijima, S. *Angew. Chem., Int. Ed.* **2011**, *50*, 4853.
- (27) Son, Y. W.; Cohen, M. L.; Louie, S. G. *Phys. Rev. Lett.* **2006**, *97*.
- (28) Louie, S. G.; Son, Y. W.; Cohen, M. L. *Nature* **2006**, *444*, 347.
- (29) Chuvilin, A.; Bichoutskaia, E.; Gimenez-Lopez, M. C.; Chamberlain, T. W.; Rance, G. A.; Kuganathan, N.; Biskupek, J.; Kaiser, U.; Khlobystov, A. N. *Nat. Mater.* **2011** advanced on line publication.